

Wideband-Notched Miniaturized UWB Polygon-Slot Antenna Using Rectangular CSRR

Bihui Xu^{1, 2}, Yanwen Zhao^{1, *}, Yuteng Zheng¹,
Li Gu¹, Qiangming Cai¹, and Zaiping Nie¹

Abstract—A miniaturized planar ultra-wideband (UWB) polygon-slot antenna with wideband-notched property is presented in this paper. With coplanar waveguide (CPW)-fed structure and miniaturized dimensions of $18.5 \times 20.5 \text{ mm}^2$, the antenna is easy to be integrated with microwave circuitry. By using one rectangular CSRR on rectangular patch, the WLAN band from 4.8 to 5.9 GHz is rejected. By cutting off two small rectangles in the lower corners of the rectangular patch, Antenna 2 is finally proposed, and UWB impedance matching from 3.1 to 12.6 GHz is achieved. The final proposed antenna is fabricated on a low-cost FR4 substrate and measured, and the measured and simulated results show an acceptable agreement. The antenna is validated to perform good radiation properties such as nearly stable radiation patterns, high gain, and high radiation efficiency.

1. INTRODUCTION

Ultra-wideband (UWB) technology has become a good candidate in various wireless communication applications with its high data transmission rates, low cost for short range communication, low complexity, low power density, and very low interference [1]. Among wireless communication systems, antenna is one of the main issues, hence good performance of UWB antennas is significant for UWB systems. An excellent UWB antenna designing should generally have remarkable performances on UWB impedance matching, radiation stability, compact appearance, cheap manufacturing, etc. In recent years, miniaturized UWB antennas have also been extensively employed in microwave imaging applications and wireless sensor networks, e.g., a miniaturized metamaterial (MTM) UWB antenna was proposed in [2]. Moreover, it is often easy to fabricate planar antennas into monolithic microwave integrated circuits (MMICs). Thus, designing miniaturized and low profile UWB antennas has attracted great interest from many researchers both in academia and industry communities of telecommunications.

Among planar UWB antenna designs in the literature, most attention is focused on planar monopole antennas and planar wide-slot antennas [2–17]. The advantages of a planar wide-slot antenna include wide bandwidth performance, compactness, and low cost in the printed circuit board (PCB) process. Based on the electromagnetic theory, impedance bandwidth and radiation efficiency can be enhanced when the slot of wide-slot antenna widens. And wide-slot antennas can be more compact by choosing proper slot and radiating patch shapes with optimized dimensions. Therefore, this paper chooses planar wide-slot antenna to design one miniaturized UWB antenna. Besides, UWB communication systems occupy a frequency band of 3.1–10.6 GHz approved by Federal Communications Commission (FCC) in 2002, overlap with several existing narrowband wireless communication systems, such as IEEE 802.11 wireless local area network (WLAN) and WiMAX. Thus, there is a great demand for designing UWB antennas with band notch to avoid or minimize potential interferences. Many approaches have been

Received 8 February 2019, Accepted 15 April 2019, Scheduled 13 May 2019

* Corresponding author: Yanwen Zhao (ywzhao@uestc.edu.cn).

¹ School of Electronic Science and Engineering, University of Electronic Science and Technology of China, Chengdu, China. ² Information Engineering College, Jimei University, Xiamen, China.

developed for planar UWB antennas with band-notched or multiple-band-notched property, e.g., by etching different types of slots on the patches, ground planes or feed lines, or by loading parasitic structures [4–8, 10, 12, 13, 16]. However, among those designs, only a narrowband notch is achieved by using one slot or inclusion, or using one pair of split-ring resonators (SRRs) coupled to the feed line [4, 6–8]. In addition, the latter method limits miniaturization of UWB antenna. Moreover, currently IEEE 802.11ac WLAN occupies a band of 5.15–5.825 GHz, hence the demand for wideband notch design increases. As reported in [5], wideband notch is obtained by using dual pairs of SRRs while their resonance frequencies are close. In the design, the SRRs are required to be placed symmetrically on the back side of the planar monopole antenna along the coplanar waveguide (CPW) feed line. However, it is generally difficult to make their centers precisely coincide with the slot lines of the CPW feed. This paper proposes a method to realize wideband notch easily, and the size of the proposed antenna can be further reduced with the band notch structure.

In this paper, a miniaturized CPW-fed UWB polygon-slot antenna is presented, and one rectangular complementary SRR (CSRR) or slot-type SRR is adopted on a rectangular patch to achieve wideband-notched property. This paper extends our previous work presented in [18] to further reduce the antenna's size and obtain better performance of the UWB antenna. The rectangular patch is modified to truncated rectangular patch in order to broaden matched impedance bandwidth. These two antennas with different patches are titled as antenna 1 and antenna 2, respectively. Both of them have promising performance on the UWB impedance matching and radiation patterns over the entire UWB band with WLAN wideband-notched property. Table 1 shows comparison of several recently presented UWB antennas with the proposed antenna in terms of size, bandwidth, gain, and band notch property. By comparison, the size of the proposed UWB antenna is relatively smaller; its impedance bandwidth is wider; and the gain is relatively higher.

Table 1. Comparison of several UWB antennas with the proposed antenna.

Reference number	Dimensions (mm ²)	Bandwidth (GHz)	Maximum gain (dBi)	Band notched property (GHz)
[4]	50 × 50	2.6–10.8	4	yes, narrow
[5]	50 × 50	2.6–10.8	4	yes, 0.7
[6]	24 × 34.6	3.1–10.6	4.5	yes, narrow
[8]	24 × 25	3.05–14.2	4.5	yes, narrow
[9]	22 × 24	3–11.2	5.4	no
[10]	25 × 28	3–11	3.8	yes, narrow
[14]	20 × 25	3–12.08	5	no
This work antenna 1 antenna 2	18.5 × 20.5	3.1–11.2	6.2	yes, 1.1
	18.5 × 20.5	3.1–12.6	6.2	yes, 1.1

The remainder of this paper is organized as follows. Section 2 outlines the designing process of miniaturized UWB slot antenna and investigates the characteristics of rectangular SRR. Section 3 presents the results and discussions of the UWB slot antenna. Section 4 gives a brief conclusion.

2. ANTENNA DESIGNS

2.1. The UWB Polygon-Slot Antenna with Rectangular Patch

In this section, the planar UWB polygon-shaped slot antenna with rectangular patch is firstly proposed. Its geometry and configuration is shown in Fig. 1. It consists of a polygon aperture etched out from the ground plane and a 50 Ω CPW-fed rectangular patch. The slot etched out from ground plane has strong coupling to the feeding structure. Due to lower radiation loss and less dispersion than microstrip lines,

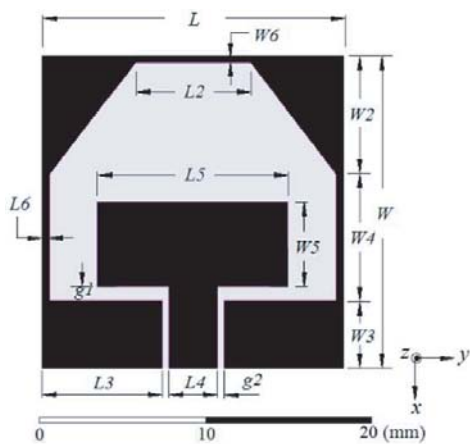


Figure 1. Configuration of the UWB polygon-slot antenna with rectangular patch.

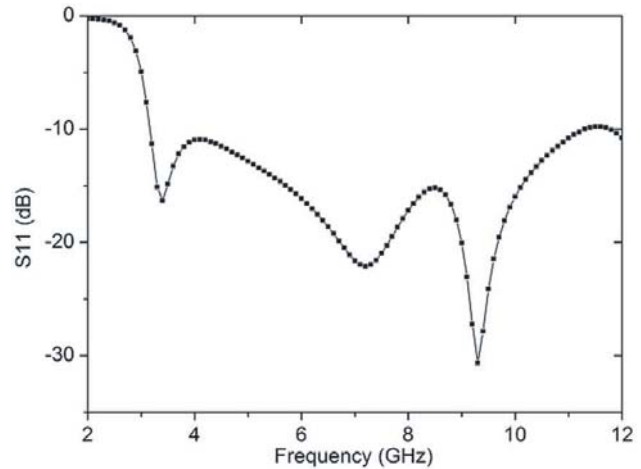


Figure 2. Simulated return loss S_{11} of the UWB polygon-slot antenna with rectangular patch.

the CPW feed line is preferred in designing UWB antenna. The printed antenna is designed on a low cost FR-4 epoxy substrate of thickness 1.6 mm and permittivity 4.4. The commercial software HFSS is employed to perform the design and optimization process. The gap between the signal strip and the finite coplanar ground plane is 0.4 mm, and the gap between the stub and the ground plane is tuned to 0.9 mm to get good impedance matching.

By tuning the shape of slot to polygon, which adds one edge L_2 based on the taper-shaped slot with the same overall dimensions, the lowest frequency f_L of the antenna impedance bandwidth gets lower than that of the latter, because the lowest frequency is specified by the longest electrical length or the longest current path, and the electrical length of polygon slot is longer than that of taper slot. Then L_2 is tuned to 7 mm, and f_L equals the lower start frequency of the UWB band. Choosing the patch shape as rectangle, its matched impedance bandwidth with $S_{11} < -10$ dB is wider than that of other shapes, such as taper, circle, and square, for the highest frequency is specified by the dimensions of patch, especially the width of patch. Then carefully tuning the width W_2 of the slot, width W_5 , and length L_5 of the patch, the antenna is optimized to have 10 dB return loss bandwidth from 3.1 to 11.2 GHz, as depicted in Fig. 2. In order to cover the entire UWB, the overall dimensions of the antenna are tuned to 19×21 mm². However, while rectangular CSRR is used on rectangular patch to achieve band notch, the antenna can be more compact but retaining the same matched impedance bandwidth. It will be discussed in Subsection 2.2.

2.2. Antenna with Rectangular CSRR on Rectangular Patch

Figure 3(a) shows the geometry of the rectangular SRR which consists of two concentric split rectangular metallic rings and gaps appearing on opposite sides. SRR has been extensively used as a metamaterial (MTM) unit cell with negative effective permeability, which is originally proposed by Pendry et al. [19]. It exhibits negative permeability when a magnetic field perpendicular to the structure is applied. According to Smith inversion algorithm in [20–22] and by using HFSS and MATLAB, the effective material parameters of rectangular SRR are extracted, as shown in Fig. 4. The simulated parameters of the rectangular SRR are $L_7 = 7.8$ mm, $W_7 = 5.1$ mm, $d_1 = 0.2$ mm, $d_2 = 0.3$ mm, $g = 0.4$ mm, the same as the optimized parameters of the CSRR listed in Subsection 2.3. It can be found from the figure that the effective permeability of the SRR is negative, and permittivity is positive roughly between 2.5 GHz and 2.75 GHz. It is obviously a sub-wavelength resonance structure. By tuning length L_7 or width W_7 of the SRR, or thickness d_1 of the metallic rings, the negative permeability band can be adjusted. Adjusting the width of the metallic rings d_2 or the split gap g has little effect on the offset of the band.

Because of the sub-wavelength resonance property and high quality factor, SRRs and their complementary structures have been well used in designing planar UWB antennas with band notch.

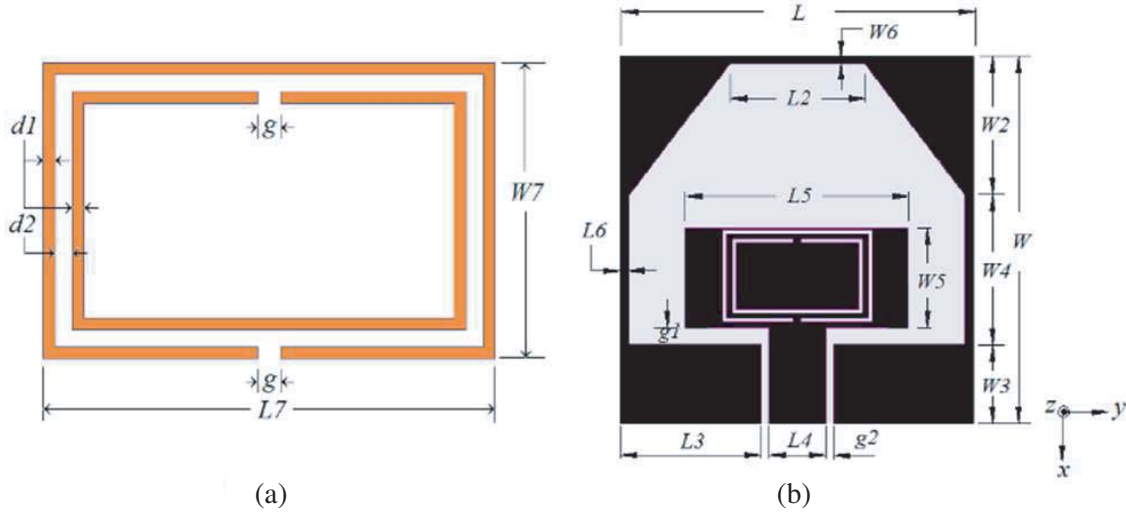


Figure 3. (a) Geometry of rectangular SRR, (b) configuration of antenna 1.

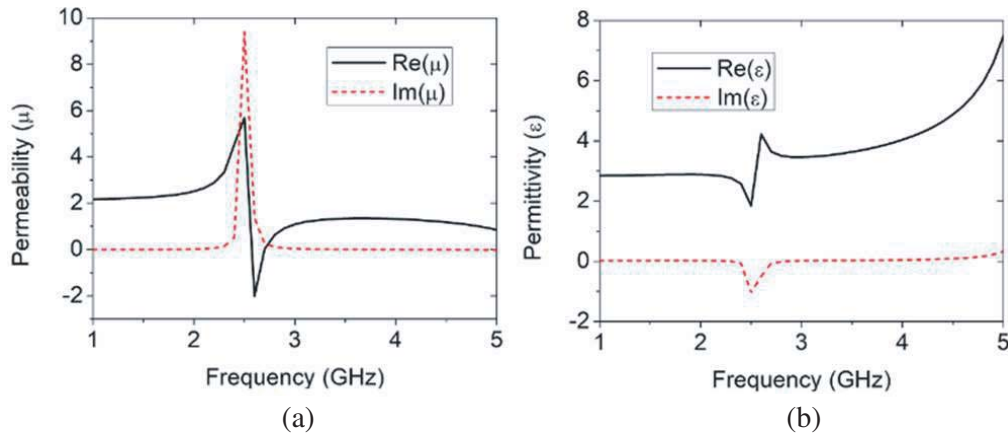


Figure 4. Retrieved material parameters of rectangular SRR, (a) permeability μ , (b) permittivity ε .

In our design, CSRR is preferably used on the patch to miniaturize the UWB antenna. Most SRRs and CSRRs in the literature are circular or square in shape. Considering that the patch shape of the proposed antenna is rectangle, the CSRR is modified to a similar rectangle for generating stronger resonance and being easy to get wideband notch covering the complete band of IEEE 802.11ac WLAN. The reason is that the shape of the CSRR is similar to that of the patch, and the current concentrates at the edge of the patch.

By using one rectangular CSRR on a rectangular patch, wideband-notched property of the UWB antenna is achieved. Fig. 3(b) shows the configuration of antenna 1 in which one rectangular SRR is etched on a rectangular patch. The CSRR is oriented in the center of the patch, and the gap between the upper edge of the CSRR and upper edge of the patch is 0.1 mm. Based on the dimensions of square SRR and its frequency in [20], the size of the rectangular CSRR is preliminarily determined. Then the desired resonance frequency within WLAN band is obtained by simulation optimization. Through electromagnetic (EM) simulation, it is found that increasing the width W_7 of rectangular CSRR results in lower resonance frequency and slightly narrower bandwidth of band notch, as shown in Fig. 5. Lengthen the length L_7 of rectangular CSRR, the resonance frequency is also reduced, but bandwidth of band notch almost does not change, as shown in Fig. 6. By analysis, the resonance frequency is inversely proportional to the width and length of the CSRR, but it cannot be calculated by empirical formula suitable for single split ring slot, whereas increasing thickness d_1 of the rings, the

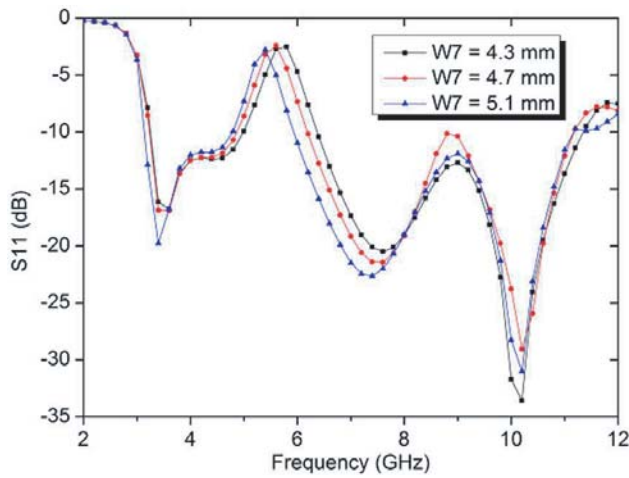


Figure 5. Effects of the width W_7 of rectangular CSRR on the notch frequency with optimal dimension of the length $L_7 = 7.8$ mm.

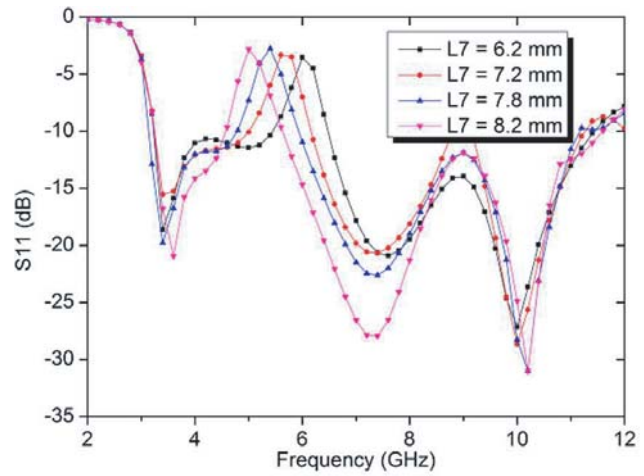


Figure 6. Effects of the length L_7 of rectangular CSRR on the notch frequency with optimal dimension of the width $W_7 = 5.1$ mm.

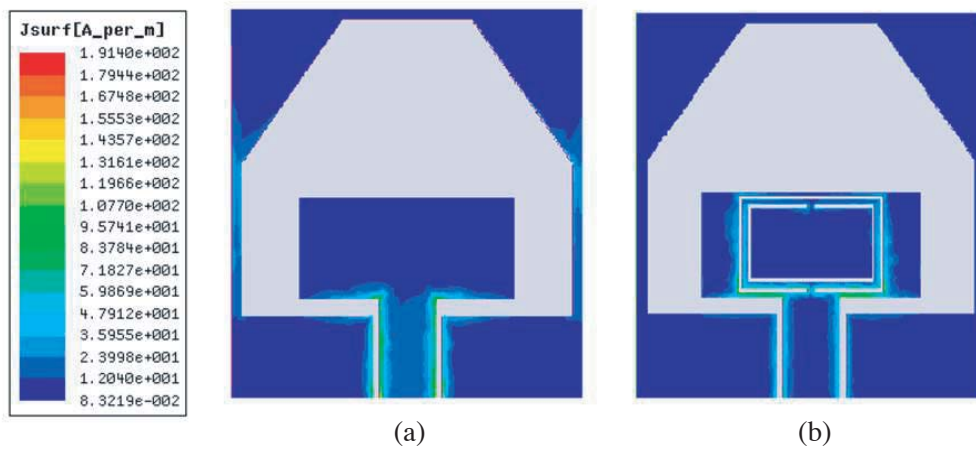


Figure 7. Current distributions at 4 GHz, (a) antenna without rectangular CSRR on rectangular patch, (b) antenna 1.

notch frequency moves towards high frequency band. The results are consistent with the analysis of characteristics of rectangular SRR described above. It is easy to get flexible frequency notch property by using rectangular CSRR. The method provides three degrees of freedom for designing UWB antennas with band notch, i.e., length and width of rectangular CSRR, and thickness of the rings.

Furthermore, through HFSS simulation, it is noted that the current concentrates around the middle and bottom parts of rectangular patch, as shown in Fig. 7(a). Then the proper rectangular SRR etched on rectangular patch makes the current distribution concentrate on two sides and bottom of the patch, which improves impedance matching indirectly, as shown in Fig. 7(b). It can be seen from Fig. 7(b) that rectangular patch etching rectangular SRR is approximately equivalent to a fork-shaped patch. Slot antennas with fork-shaped patch have significant enhancement on impedance bandwidth compared to the same slot antennas with rectangular patch [15]. Therefore, it is used to further reduce the antenna's size while keeping the lowest frequency of the UWB band constant. This feature is not available in circular SRR etched on the patch. In the end, the rectangular CSRR is optimized to satisfy resonance frequency within WLAN band and obtain wider matched impedance bandwidth. The overall dimensions

of antenna 1 are optimized to $18.5 \times 20.5 \text{ mm}^2$, smaller than most miniaturized UWB antennas mentioned in [2–17], and some of them do not provide band-notched property.

2.3. Antenna with Truncated Rectangular Patch

To further broaden the bandwidth of the UWB antenna, antenna 2 is proposed. Fig. 8 shows the configuration and photograph of fabricated antenna 2. Antenna 2 is based on antenna 1 by cutting off two small rectangles in the lower corners of the rectangular patch, as shown in Fig. 8(a). The method that truncating two lower corners of the patch can improve higher frequencies impedance matching condition. It is worth of noting that impedance matching characteristic of one pair of rectangular notches on the patch is better than that of one pair of triangular notches for the polygon-slot antenna. Tuning the length d_3 and width d_4 of the rectangular notches to proper size of 1.9 mm and 0.5 mm, respectively, antenna 2 provides broader matched impedance bandwidth than antenna 1 with acceptable radiation properties and high efficiency.

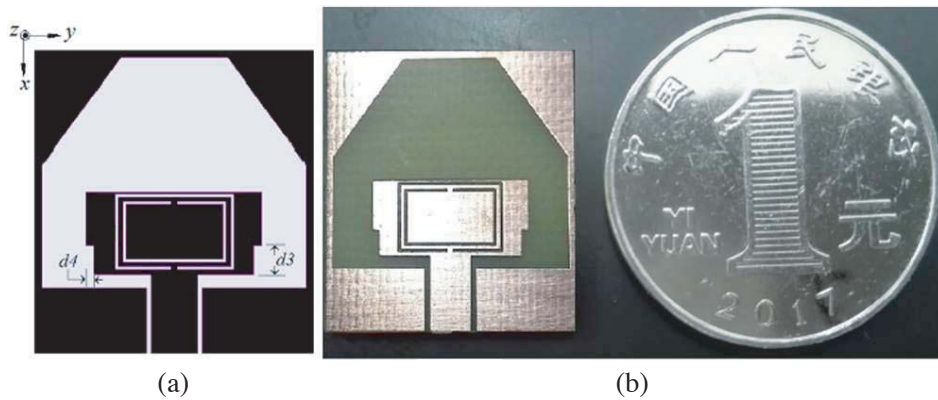


Figure 8. (a) Configuration of antenna 2, (b) photograph of fabricated antenna 2.

The optimized design parameters of the prototype antenna are $L = 18.5 \text{ mm}$, $W = 20.5 \text{ mm}$, $L_2 = 7 \text{ mm}$, $L_3 = 7.35 \text{ mm}$, $L_4 = 3 \text{ mm}$, $W_2 = 7.8 \text{ mm}$, $W_3 = 4.5 \text{ mm}$, $W_4 = 8.2 \text{ mm}$, $L_5 = 11.6 \text{ mm}$, $W_5 = 5.5 \text{ mm}$, $L_6 = 0.5 \text{ mm}$, $W_6 = 0.5 \text{ mm}$, $g_1 = 0.9 \text{ mm}$, $g_2 = 0.4 \text{ mm}$, $h = 1.6 \text{ mm}$. The optimized parameters of CSRR are $L_7 = 7.8 \text{ mm}$, $W_7 = 5.1 \text{ mm}$, $d_1 = 0.2 \text{ mm}$, $d_2 = 0.3 \text{ mm}$, $g = 0.4 \text{ mm}$.

3. RESULTS AND DISCUSSION

In our simulation process, HFSS is employed. The current distributions of antenna 2 at 5.3 GHz and 7 GHz are respectively plotted in Fig. 9. It can be found that the current concentrates around the CSRR at 5.3 GHz, but the presence of the CSRR has little influence on current distributions at other frequencies, e.g., 7 GHz. This is because the propagating EM signal excites the CSRR resonance at around 5.3 GHz. The resonance prohibits radiation, then achieves a notch nearby. Next, the simulated return losses of antenna 1 and antenna 2 are shown in Fig. 10. The impedance bandwidth of antenna 1 with $S_{11} < -10 \text{ dB}$ rejecting WLAN band is from 3.1 to 11.2 GHz. Antenna 2 provides fractional bandwidth of 121% ranging from 3.1 to 12.6 GHz. It can be observed that the low frequency impedance performances for them are the same. However, at high frequency band, the return loss of antenna 2 increases, then the highest frequency of impedance bandwidth increases. Moreover, there is an obvious resonance at 5.3 GHz, and the notched band is from 4.8 to 5.9 GHz. The wideband-notched property is finally obtained by using only one rectangular CSRR on a rectangular patch.

Antenna 2 is fabricated on an FR4 substrate and measured in an anechoic chamber. A photograph of antenna 2 is shown in Fig. 8(b). Seeing from the spectrum of impedance performance given in Fig. 10, there are three resonances around the frequencies at 4, 7.6, and 10 GHz. The measurement is in agreement with simulation, but the measured impedance bandwidth is from 3.1 to 10.7 GHz, which

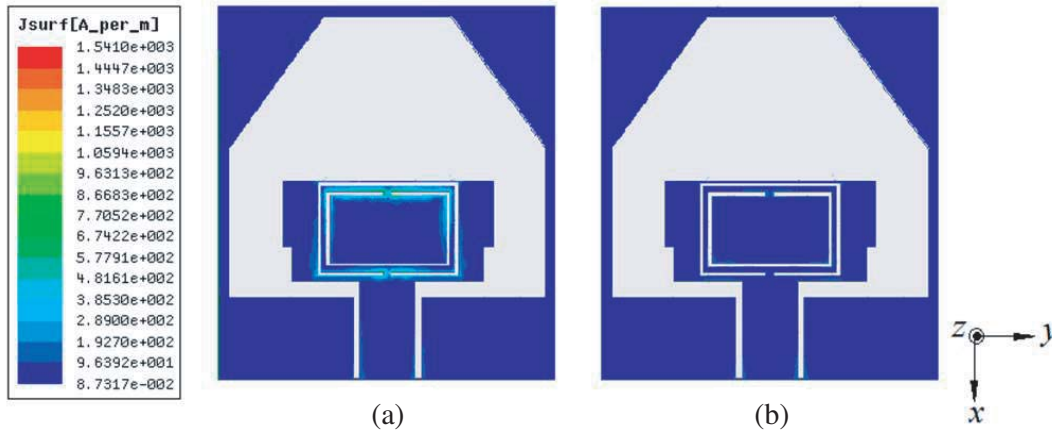


Figure 9. Current distributions of antenna 2 at different frequencies, (a) 5.3 GHz, (b) 7 GHz.

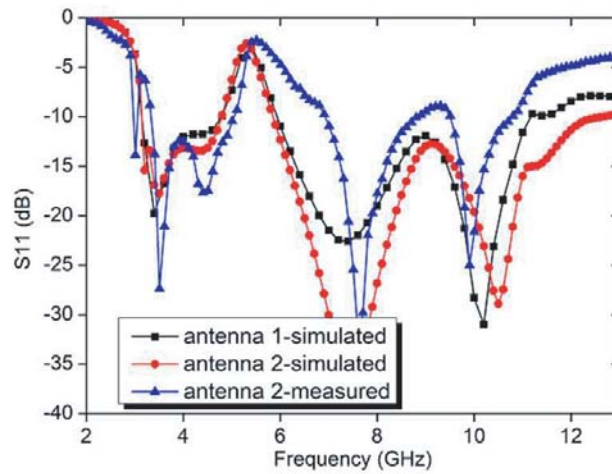


Figure 10. Simulated return loss S_{11} of antenna 1, measured and simulated return loss S_{11} of antenna 2.

is narrower than that of the simulated result. The main cause of the discrepancy is the unstable FR4 relative permittivity. Fig. 11 shows the simulated and measured far field radiation patterns of antenna 2 in the xz -plane (E -plane) and yz -plane (H -plane), respectively at 4 GHz, 7.6 GHz, and 10 GHz. The simulated radiation patterns in the E -plane are eight shape, while the simulated radiation patterns in the H -plane are omnidirectional. As frequency moves toward the upper end of the impedance bandwidth, the radiation patterns are somewhat distorted. There is a little disagreement between simulation and measurement at 4 GHz, but they show acceptable agreements at 7.6 and 10 GHz. The disagreement between simulation and measurement is mainly due to the fabrication tolerance and measurement environment. And the relatively large discrepancy at 4 GHz is also due to the small ground plane size, so a few leakage currents may distribute along the external conductor of the SMA connector and may affect the radiation patterns.

As depicted in Fig. 12, the simulated radiation peak gain of antenna 2 rejecting WLAN band varies from 2.7 to 6.2 dBi and significantly decreases at 4.8 to 5.9 GHz over the notched band. Its maximum gain of 6.2 dBi is higher than those antennas described in Table 1. It is also found that the measured radiation peak gain agrees well with the simulated results, but a little higher than the simulation in the middle and low frequency bands. The main reason is, as mentioned above, that the small size and low gain antenna is easy to be influenced by measurement environment, especially at lower frequencies, and its measurement error is relatively high. Moreover, the simulated radiation efficiency of antenna 2 rejecting WLAN band is over 84%, as shown in Fig. 13.

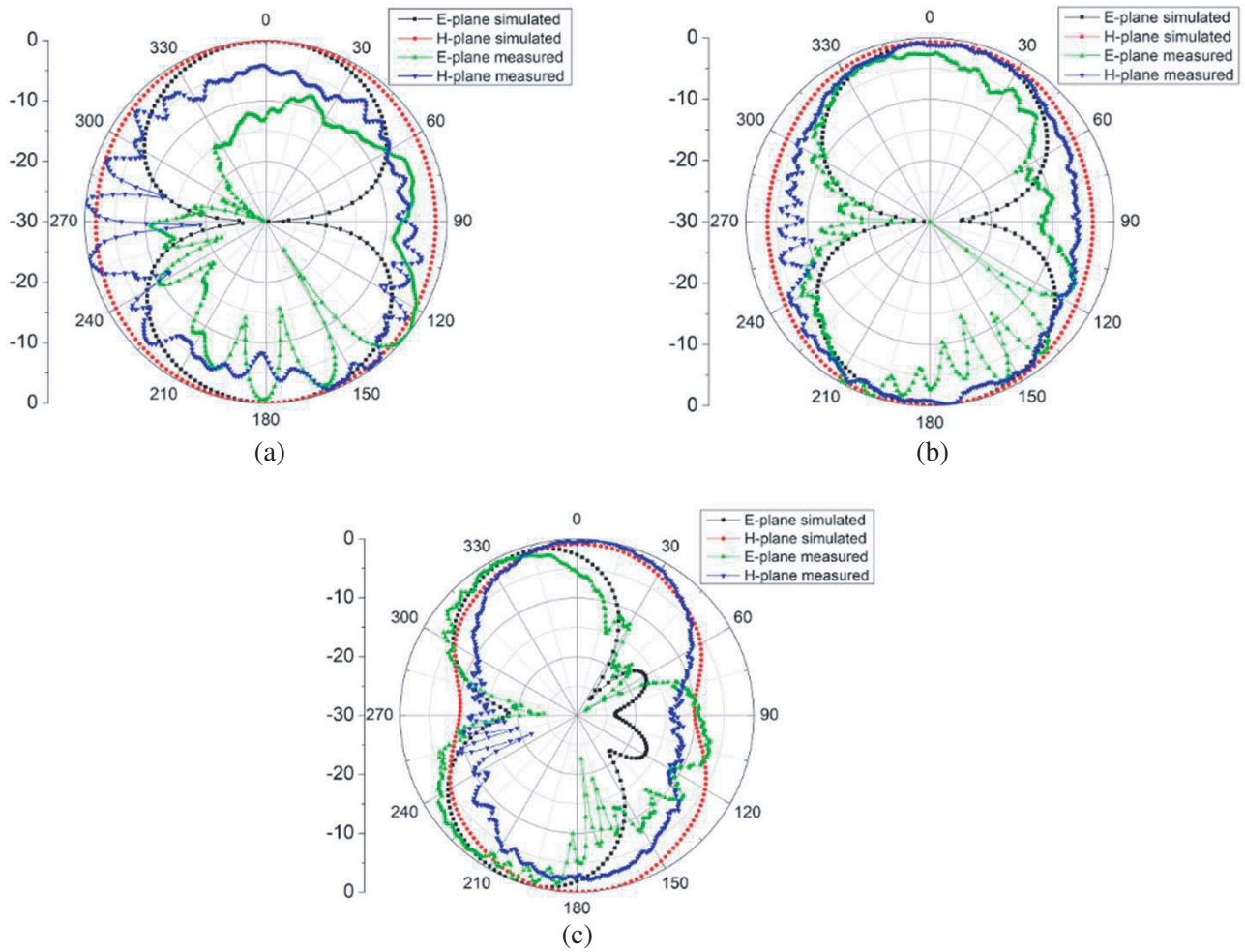


Figure 11. Simulated and measured radiation patterns at (a) 4 GHz, (b) 7.6 GHz, (c) 10 GHz.

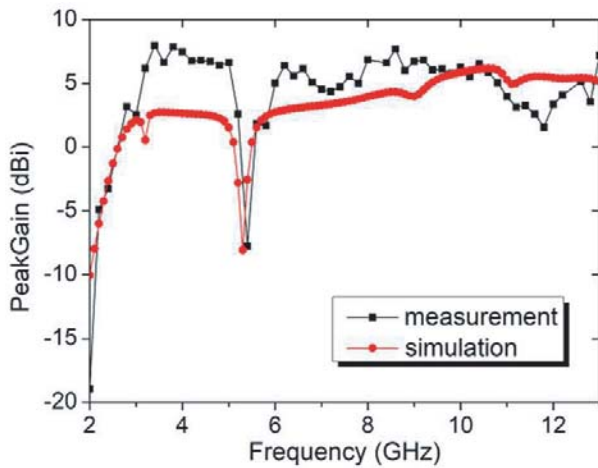


Figure 12. Measured and simulated radiation peak gain of antenna 2.

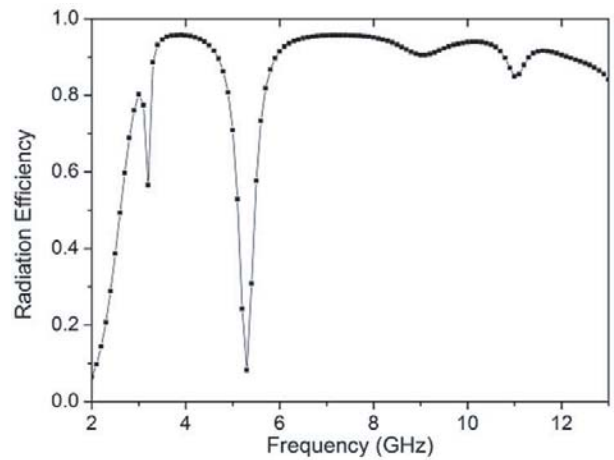


Figure 13. Simulated radiation efficiency of antenna 2.

4. CONCLUSION

By using one rectangular CSRR, a miniaturized CPWfed UWB polygon-slot antenna with WLAN wideband-notched property ranging from 4.8 to 5.9 GHz is designed in this paper. In our design, the overall dimensions of the antenna are only $18.5 \times 20.5 \text{ mm}^2$. With a CPW-fed structure and compact size, this design is easy to fabricate, and the rectangular SRR etched on a similar shape patch can also enhance the impedance matching indirectly. The final proposed antenna, i.e., antenna 2, provides the matched impedance bandwidth of 121% ranging from 3.1 to 12.6 GHz rejecting WLAN band. It achieves a maximum gain of 6.2 dBi at 10.5 GHz, high radiation efficiency over 84%, and nearly stable radiation patterns. Antenna 2 is fabricated on a low cost FR4 substrate and measured, and the measured and simulated results show an acceptable agreement in terms of return loss, radiation pattern, and gain.

ACKNOWLEDGMENT

The authors thank the National Natural Science Foundation of China under Grant No. 61371050 and No. 61721001, and the Natural Science Foundation of Fujian Province under Grant No. 2018J01540.

REFERENCES

1. Sibal, V., B. Allen, D. Edwards, and B. Honary, "Twenty years of ultrawideband: Opportunities and challenges," *IET Commun.*, Vol. 6, No. 10, 1147–1162, Jul. 2012.
2. Islam, M. M., M. T. Islam, M. Samsuzzaman, et al., "A miniaturized antenna with negative index metamaterial based on modified SRR and CLS unit cell for UWB microwave imaging applications," *Materials*, Vol. 8, No. 2, 392–407, Feb. 2015.
3. Gupta, A. and R. K. Chaudhary, "A compact CPW-fed wideband metamaterial antenna with EBG loading," *Microwave Opt. Technol. Lett.*, Vol. 57, No. 11, 2632–2636, Nov. 2015.
4. Siddiqui, J. Y., C. Saha, and Y. M. M. Antar, "Compact SRR loaded UWB circular monopole antenna with frequency notch characteristics," *IEEE Trans. Antennas Propag.*, Vol. 62, No. 8, 4015–4020, Aug. 2014.
5. Siddiqui, J. Y., C. Saha, and Y. M. M. Antar, "Compact dual-SRR-loaded UWB monopole antenna with dual frequency and wideband notch characteristics," *IEEE Antennas Wireless Propag. Lett.*, Vol. 14, 100–103, 2015.
6. Sarkar, M., S. Dwari, and A. Daniel, "Printed monopole antenna for ultra-wideband application with tunable triple band-notched characteristics," *Wireless Pers. Commun.*, Vol. 84, 2943–2954, 2015.
7. Zhang, Y., W. Hong, C. Yu, et al., "Planar ultrawideband antennas with multiple notched bands based on etched slots on the patch and/or split ring resonators on the feed line," *IEEE Trans. Antennas Propag.*, Vol. 56, No. 9, 3063–3068, Sep. 2008.
8. Li, L., Z. L. Zhou, Z. S. Hong, and B. Z. Wang, "Compact dual-band-notched UWB planar monopole antenna with modified SRR," *Electronics Letters*, Vol. 47, No. 17, Aug. 2011.
9. Azim, R., M. T. Islam, and N. Misran, "Compact tapered-shape slot antenna for UWB applications," *IEEE Antennas Wireless Propag. Lett.*, Vol. 10, 1190–1193, 2011.
10. Eshtiaghi, R., J. Nourinia, and C. Ghobadi, "Electromagnetically coupled band-notched elliptical monopole antenna for UWB applications," *IEEE Trans. Antennas Propag.*, Vol. 58, No. 4, 1397–1402, Apr. 2010.
11. Ellis, M. S., Z. Zhao, J. Wu, et al., "Small planar monopole ultra-wideband antenna with reduced ground plane effect," *IET Microw. Antennas Propag.*, Vol. 9, 1028–1034, 2015.
12. Chu, Q.-X. and Y.-Y. Yang, "A compact ultrawideband antenna with 3.4 ~ 5.5 GHz dual band-notched characteristics," *IEEE Trans. Antennas Propag.*, Vol. 56, No. 12, 3637–3644, Dec. 2008.
13. Lin, Y.-C. and K.-J. Hung, "Compact ultrawideband rectangular aperture antenna and band-notched designs," *IEEE Trans. Antennas Propag.*, Vol. 54, No. 11, 3075–3081, Nov. 2006.

14. Chakraborty, M., S. Pal, and N. Chottoraj, "Realization of high performance compact CPW-fed planar UWB antenna using higher order asymmetry for practical applications," *Microwave Opt. Technol. Lett.*, Vol. 58, No. 2, 2515–2519, 2016.
15. Sze, J. Y. and K. L. Wong, "Bandwidth enhancement of a microstrip-line-fed printed wide-slot antenna," *IEEE Trans. Antennas Propag.*, Vol. 49, 1020–1024, 2001.
16. Shrikanth Reddy, G., A. Kamma, S. K. Mishra, and J. Mukherjee, "Compact bluetooth/UWB dual-band planar antenna with quadruple band-notch characteristics," *IEEE Antennas Wireless Propag. Lett.*, Vol. 13, 872–875, 2014.
17. Narbudowicz, A., M. John, V. Sipal, X. Bao, and M. J. Ammann, "Design method for wideband circularly polarized slot antennas," *IEEE Trans. Antennas Propag.*, Vol. 63, No. 10, 4271–4279, 2015.
18. Xu, B., Y. Zhao, Y. Zheng, and L. Gu, "Compact UWB slot antenna with wideband-notched characteristics based on rectangular SRR," *2016 5th IEEE Asia-Pacific Conference on Antennas and Propagation, Conference Proceedings*, 29–30, Feb. 2017.
19. Pendry, J. B., et al., "Magnetism from conductors and enhanced nonlinear phenomena," *IEEE Trans. Micr. Theory Tech.*, Vol. 47, No. 11, 2075–2084, Nov. 1999.
20. Smith, D. R. and S. Schultz. "Determination of effective permittivity and permeability of metamaterials from reflection and transmission coefficients," *Phy. Rev. B*, Vol. 65, 195104, 2002.
21. Smith, D. R., D. C. Vier, Th. Koschny, and C. M. Soukoulis, "Electromagnetic parameter retrieval from inhomogeneous metamaterials," *Phys. Rev. E*, Vol. 71, 036617, 2005.
22. Chen, X., T. M. Grzegorzcyk, B.-I. Wu, et al., "Robust method to retrieve the constitutive effective parameters of metamaterials," *Phys. Rev. E*, Vol. 70, 016608, 2004.